Proc. Natl. Acad. Sci. USA
Vol. 85, pp. 9336–9340, December 1988
Neurobiology

Patch-clamp study of γ-aminobutyric acid receptor Cl^- channels in cultured astrocytes

(glia/benzodiazepine/ion channel)

JOACHIM BORMANN*† AND HELMUT KETTENMANN‡

*Max-Planck-Institut für biophysikalische Chemie, Am Fassberg, D-3400 Göttingen, Federal Republic of Germany; and ‡Institut für Neurobiologie, Universität Heidelberg, Im Neuenheimer Feld 504, D-6900 Heidelberg, Federal Republic of Germany

Communicated by Gerald D. Fischbach, August 22, 1988

ABSTRACT **The membrane channels operated by γ-aminobutyric acid (GABA) were studied in cultured astrocytes from rat cerebral hemispheres by using patch-clamp techniques. The channel properties appeared to be very similar, in many respects, to those present in neuronal cell membranes. The Cl^--selective channels were activated after the sequential binding of two GABA molecules to the receptor, as deduced from the slope of the dose–response curve. Single-channel currents displayed multiple conductance states of 12 pS, 21 pS, 29 pS, and 43 pS, with the main-state conductance being 29 pS. The gating properties could be described by a sequential reaction scheme for agonist-activated channels. GABA-induced whole-cell currents were potentiated by the benzodiazepine receptor agonist diazepam and also, to a lesser extent, by methyl 6,7-dimethoxy-4-ethyl-β-carboline-3-carboxylate, an inverse agonist. In neurons and chromaffin cells, methyl 6,7-dimethoxy-4-ethyl-β-carboline-3-carboxylate reduces the sensitivity of the GABA receptor, indicating that neuronal and glial GABA/benzodiazepine receptor–Cl^- channel complexes are different. Glial GABA receptor channels could be of functional importance in buffering extracellular Cl^- in the cleft of the GABAergic synapse.**

In the mammalian central nervous system γ-aminobutyric acid (GABA) is the main neurotransmitter mediating synaptic inhibition (1). The GABA-induced conductance increase of the postsynaptic membrane is caused by the opening of ionic channels selectively permeable for chloride (2). GABA-activated membrane channels have been studied in a variety of neuronal cell types by using patch-clamp techniques (for review, see ref. 3). These channels have multiple conductance states of 12 pS, 21 pS, 30 pS, and 44 pS with a main-state conductance of 30 pS (4). Currents through single GABA receptor channels occur in bursts with mean open times of 20–60 msec (5, 6). The activity of the channels is modulated by ligands that bind to the benzodiazepine receptor site associated with the GABA receptor (7). In neuronal cells, benzodiazepine receptor agonists, such as diazepam, potentiate GABA-induced membrane currents (6, 8, §) whereas inverse agonists, such as methyl 6,7-dimethoxy-4-ethyl-β-carboline-3-carboxylate (DMCM), decrease them (9).

The action of GABA in the central nervous system is not restricted to neurons. Cultured oligodendrocytes and astrocytes from various tissues and species respond to GABA with a membrane depolarization (10–12). The underlying ionic mechanism has been identified in cultured astrocytes as an increase of the membrane conductance for Cl^- (13). The glial response to GABA shares many pharmacological properties with the one mediated by the neuronal $GABA_A$ receptor. Muscimol, a $GABA_A$ receptor agonist, elicited a response similar to GABA, while baclofen, an agonist of $GABA_B$ receptors, did not induce any reaction in the astrocytes; $GABA_A$ receptor antagonists, such as bicuculline and picrotoxin, blocked the effect of GABA (12). Benzodiazepine receptor agonists and antagonists showed up further similarities to neurons, whereas the action of inverse agonists revealed differences between neurons and glial cells (14).

In the present study, we have obtained direct evidence for the existence of GABA-activated channels in glial cells. By using patch-clamp techniques, we have compared the properties of GABA receptor channels in cultured astrocytes to those described for neurons.

MATERIALS AND METHODS

Cell Culture. Cultures of enriched astrocytes (>90%) were obtained from cerebral hemispheres of newborn Sprague–Dawley rats as described (15, 16). The cells were plated on poly(L-lysine)-coated glass coverslips and maintained in culture for 2–4 weeks prior to the use in electrophysiological experiments. Cultures contained spherically shaped cells with a diameter of 10–20 μm and also large, but flat, cells. Both cell types have been identified as astrocytes by immunocytochemistry with glial fibrillary acidic protein as a marker (11). Bovine chromaffin cells were cultured and maintained as described (6).

Electrophysiology. Cells were bathed in standard saline solution and maintained on the stage of an inverted microscope at room temperature (20–23°C). The extracellular solution was 137 mM NaCl/5.4 mM KCl/1.8 mM $CaCl_2$/1 mM $MgCl_2$/5 mM Hepes·NaOH, pH 7.4. GABA was purchased from Sigma (Taufkirchen, F.R.G.). Diazepam and DMCM were gifts from Hoffmann–La Roche (Grenzach-Wyhlen, F.R.G.) and Ferrosan (Soeborg, Denmark), respectively.

Drugs were applied in standard solution to single cells and membrane patches by using a fast-application system: a U-shaped glass capillary tube with an outlet hole of ≈100 μm in diameter was placed next to the cell. A perfusion pump controlled the rate of flow through the U-tube (0.1 ml/min). The bathing solution could be exchanged within 100 msec by operating a magnetic valve controlling the outflow of the solution (ref. 17 and see also ref. 6).

We used the whole-cell and the outside-out patch configurations of the patch-clamp technique (18). Recordings were obtained by using hard glass pipettes (Pyrex) with resistances of 3–10 MΩ. The intracellular pipette solution was 120 mM CsCl/20 mM tetraethylammonium chloride/1 mM $CaCl_2$/2 mM $MgCl_2$/11 mM EGTA/10 mM Hepes·NaOH, pH 7.4. We recorded current and voltage signals from the patch-clamp

The publication costs of this article were defrayed in part by page charge payment. This article must therefore be hereby marked "*advertisement*" in accordance with 18 U.S.C. §1734 solely to indicate this fact.

Abbreviations: GABA, γ-aminobutyric acid; DMCM, methyl 6,7-dimethoxy-4-ethyl-β-carboline-3-carboxylate.

†To whom reprint requests should be sent at the present address: Merz & Co., Eckenheimer Landstrasse 100-104, D-6000 Frankfurt, F.R.G.

§Bormann, J. & Sakmann, B., 9th International Congress of Pharmacology, July 29–Aug. 3, 1984, London, p. S13–S14.

amplifier (EPC-7, List Electronic, Darmstadt, F.R.G.) on video tape.

Data Analysis. Current recordings from single channels were digitized at 0.4-msec intervals after low-pass filtering at 1 kHz (−3 dB). Measurements of current amplitudes and single-channel open and closed times were made on the screen of a PDP 11/23 laboratory computer system by using a semiautomatic procedure (see ref. 19). Subconductance states were distinguished from overlaps of more than one channel opening by their occurrence within bursts. For gating analyses we selected patches where only the main-state conductance was present. Whole-cell recordings of cell current were filtered at 50 Hz and plotted on an *x–y* recorder from a digital oscilloscope.

RESULTS

Whole-Cell Currents. Fig. 1*A* shows whole-cell recordings from two astrocytes clamped at a membrane potential of −70 mV. The inward currents were induced by the application of 50 μM GABA in standard saline. With our pipette solution, Cl^- distributed evenly across the membrane at a concentration of 145 mM. Thus, inward currents, at negative membrane potentials, reflected the outward movement of Cl^-. In the upper trace, obtained from a small spherical astrocyte, the current developed rapidly upon the application of GABA. Flat cells in dense monolayer cultures showed a different type of behavior (Fig. 1*A*, lower trace). The time from GABA application to the peak of the GABA-induced current was significantly longer and the trace showed relatively little membrane noise. This result is most likely explained by electrical coupling between adjacent cells and/or by a diffusion barrier between the bathing solution and receptors not directly exposed to GABA.

All astrocytes tested responded to GABA. The current amplitudes, however, induced by a given GABA concentration, appeared to be quite variable from cell to cell. At 10 μM GABA, the currents ranged from 40 to 450 pA with an average of 225 ± 140 pA (mean ± SD, n = 11).

The peak amplitudes of GABA-induced whole-cell currents were concentration-dependent. Fig. 1*B* shows recordings obtained during the application of four GABA concentrations to an astrocyte clamped at a membrane potential of −70 mV. The dose–response relation is shown in Fig. 1*C* as a double-logarithmic plot of peak response vs. GABA concentration. The straight line obtained by a least-squares fit has a slope of 1.5. The average value from six cells was 1.6 ± 0.6 (mean ± SD). This result indicates that a minimum of two GABA molecules must bind to the receptor before the channel opens (5, 6).

The reversal of GABA-activated whole-cell currents was studied with extra- and intracellular Cl^- concentrations of 145 mM. Under these conditions, the average reversal potential obtained from 12 cells was −1.3 ± 2.1 mV (mean ± SD). This is close to the value of 0 mV expected with equal Cl^- concentrations on both sides of the membrane, indicating that GABA opens Cl^--specific channels.

Modulation of Cl^- Channels by Benzodiazepine Receptor Ligands. We tested the effects of diazepam, a "classical" benzodiazepine receptor agonist, on GABA-activated whole-cell currents recorded at a membrane potential of −70 mV. Fig. 2*A* shows an experiment where 20 μM GABA was applied to an astrocyte in the absence and presence of 10 μM diazepam. The GABA-induced peak current increased from the control value of 0.8 nA to 1.3 nA in the presence of diazepam. On average, GABA responses were potentiated by a factor of 1.7 ± 0.3 (mean ± SD; range, 1.5–2.2; n = 6) in the presence of 10 μM diazepam. This finding is in agreement with the results obtained for cultured neurons and chromaffin cells (6, 8, §).

An experiment with the inverse benzodiazepine receptor ligand DMCM is shown in Fig. 2*B*. This drug slightly, but consistently, augmented the GABA response of astrocytes by a factor of 1.2 ± 0.2 (mean ± SD; range, 1.0–1.5; n = 6). In neuronal cells, however, DMCM effectively decreased GABA-activated whole-cell currents (9). As a model for neurons, we used chromaffin cells where $GABA_A$ receptor channels have been well characterized (6). Fig. 2*C* shows an experiment where we applied DMCM to a bovine chromaffin cell under the experimental conditions of Fig. 2*B*. The GABA-induced current was reduced to ≈50% of control in the presence of DMCM. Thus, the GABA–benzodiazepine receptor–Cl^- channel complex seems to be different in neurons and glial cells. This is in line with the enhancement by DMCM of the GABA-induced depolarization in astrocytes (14).

Single-Channel Measurements. We studied single GABA-gated Cl^- channels in outside-out membrane patches that were obtained after the establishment of the whole-cell recording configuration. Fig. 3*A* shows a whole-cell current response evoked by the application 50 μM GABA to an astrocyte clamped at a membrane potential of −70 mV. Shortly afterwards, an outside-out patch was made by re-

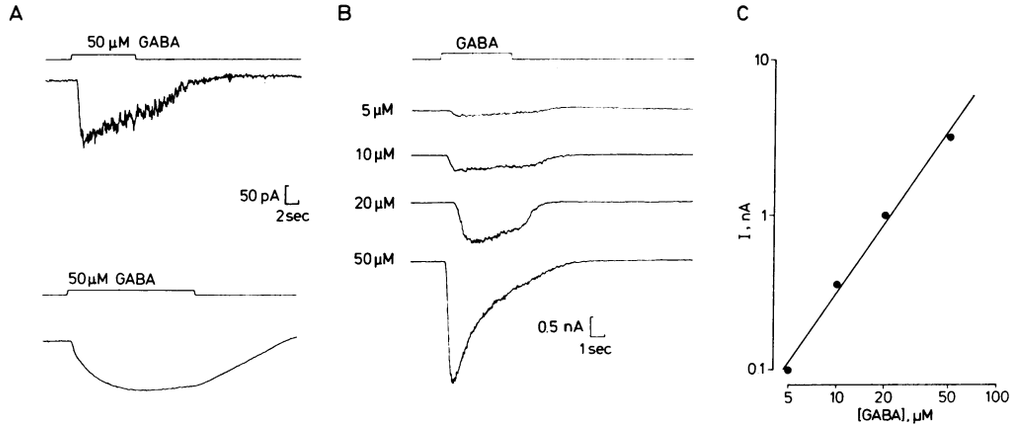

FIG. 1. Whole-cell current recording from cultured astrocytes. (*A*) GABA-induced inward currents from two cells clamped at a membrane potential of −70 mV. The upper trace is a recording from a small round astrocyte, whereas the lower trace was obtained from a flat cell in a dense monolayer culture. GABA was applied by the U-tube method, as indicated above the traces. Note the difference in the time course and membrane noise between the two recordings. The scale bar applies to both cells. (*B*) Current responses of an astrocyte to various GABA concentrations (membrane potential of −70 mV). (*C*) Dose–response curve corresponding to data in *B*. The peak response of the current (I) is plotted vs. GABA concentration on double-logarithmic scales. The linear fit of the data points yields a slope of 1.6.

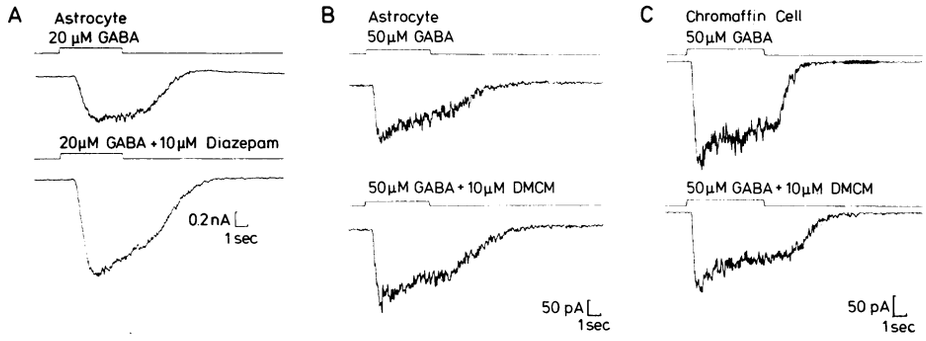

FIG. 2. Modulation of GABA receptor channels by benzodiazepine receptor ligands. (*A*) Whole-cell currents recorded from an astrocyte clamped to −70 mV. The upper trace shows an inward current triggered by 20 μM GABA. With 10 μM diazepam added to the GABA solution (20 μM), the peak current response was potentiated by a factor of 1.7. (*B*) Effect of DMCM on GABA-induced whole-cell current in an astrocyte. The response to 50 μM GABA was increased by 30% in the presence of 10 μM DMCM. (*C*) The same experimental arrangement was used to compare the effect of DMCM on GABA receptor channels in a cultured chromaffin cell. In this cell type, as in other neuronal cells, DMCM at 10 μM reduced GABA-induced whole-cell currents by ≈50%.

tracting the pipette from the cell and the GABA application was repeated (Fig. 3*B*). The openings of single GABA-activated channels were clearly resolved, with three current levels simultaneously active at the beginning of the GABA application. The overall activation pattern of currents in Fig. 3 *A* and *B* appears to be very similar except that the gain was different by a factor of 100.

The conductance of GABA-activated channels was estimated from the current–voltage relation. Fig. 3*C* shows recordings obtained from an outside-out patch at various membrane potentials. The current amplitude increased upon depolarizing or hyperpolarizing the patch from the reversal potential of 0 mV. The average single-channel current amplitude was 2.0 pA at −70 mV, resulting in a single-channel conductance of 29 pS. This is very similar to the value of 30 pS obtained for mammalian neuronal cells (4–6).

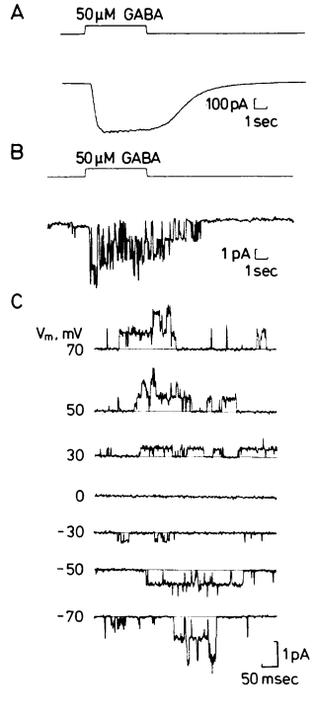

FIG. 3. Formation of an outside-out patch and recording of single-channel currents. (*A*) Whole-cell current activated by 50 μM GABA in an astrocyte held at −70 mV. (*B*) Recording of single-channel currents from an outside-out patch obtained from the cell in *A*. Note the similar time courses of currents in *A* and *B*. (*C*) Dependence of single-channel current amplitude on patch membrane potential (V_m). The current step size increased with the voltage difference from the reversal potential of 0 mV. The single-channel conductance calculated from this patch is 29 pS.

In addition to the main conductance state of 29 pS, several other less frequently occurring states were observed. A selection of recordings shown in Fig. 4*A* illustrates the multiconductance-state behavior of GABA receptor channels at −70 mV. Apart from the main current level of 2.0 pA, three other levels with mean amplitudes of 3.0 pA, 1.3 pA, and 0.85 pA are evident. The relative contribution of the four conductance levels can be assessed from the histogram in Fig. 4*B*. The current–voltage relations of the three most prominent conductance states is shown in Fig. 4*C*, in the voltage range from −90 to +90 mV. Least-squares fits yielded slope conductances of 28 pS, 21 pS, and 13 pS. In addition, a 43-pS conductance was present in this patch.

From six patches, we obtained conductance values of 29 ± 2 pS (n = 6), 21 ± 2 pS (n = 3), 12 pS (n = 2), and 43 pS (n = 1). They correspond closely to the conductance levels of GABA- and glycine-activated Cl^- channels in spinal neurons (4) and also to those of GABA receptor channels in chromaffin cells (6).

Gating Properties of GABA Receptor Channels. We also used outside-out patches to investigate the gating properties of single GABA-activated membrane channels. Fig. 5 shows the data from a patch exposed to 50 μM GABA at a membrane potential of −70 mV. The step sizes of single-channel events are uniformly distributed with a peak at 2.0 pA (Fig. 5*A*), which corresponds to a conductance of 29 pS. The distribution of closed times, shown in Fig. 5*B*, has been fitted by the sum of two exponential functions. The fast time constant of 0.8 msec reflects the average duration of the closed times (gaps) within bursts (20). The histogram of burst durations (Fig. 5*C*) has been constructed by using a critical gap duration of twice the fast constant obtained from the closed-time distribution—i.e., 1.6 msec. This distribution has also been fitted by a double-exponential function with decay time constants of 0.5 and 23.0 msec. From the ratio of long bursts to short closings, the elementary current pulse of 23 msec was on average interrupted twice by gaps of 0.8 msec—i.e., an average burst consists of three consecutive openings.

The time course of channel gating could be described by a sequential reaction scheme proposed for agonist-activated channels (ref. 21 and see also refs. 5 and 6):

$$A + R \underset{k_{-1}}{\overset{2k_1}{\rightleftharpoons}} AR + A \underset{2k_{-1}}{\overset{k_1}{\rightleftharpoons}} A_2R \underset{\alpha}{\overset{\beta}{\rightleftharpoons}} A_2R^*$$

The model predicts that two GABA molecules A bind sequentially to the receptor R to form the complex A_2R,

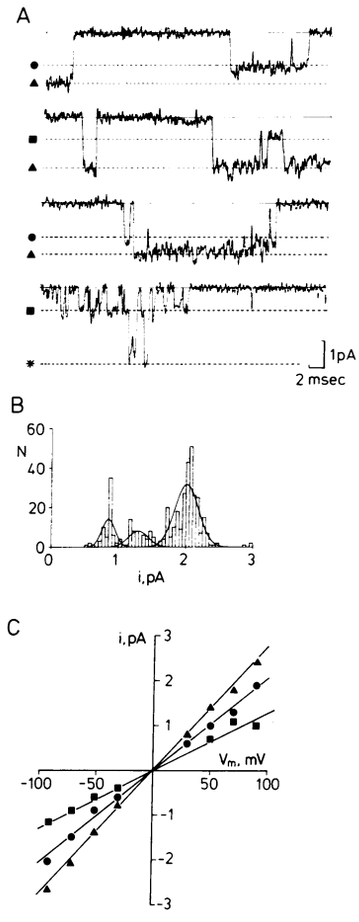

FIG. 4. Conductance states of GABA receptor channels. (*A*) Current recordings from an outside-out patch at a membrane potential of −70 mV after adding 50 μM GABA to the bath. The different current levels are marked by symbols ■, ●, ▲, and * (in an increasing order of conductance). (*B*) Amplitude histogram of currents in *A*. The three peaks were fitted by Gaussian distributions with mean amplitudes of 2.0 pA, 1.3 pA, and 0.85 pA. Rare events of a 3-pA current level were found. (*C*) Current (*i*)–voltage (V_m) relationship from the same experiment, for the three most prominent conductance levels in the membrane potential range of −90 to 90 mV. Data were linearly fitted. The slope conductances were 28 pS (▲), 21 pS (●), and 13 pS (■). The largest conductance level of 43 pS as indicated in *A* is not displayed in *C*, since openings occurred very rarely.

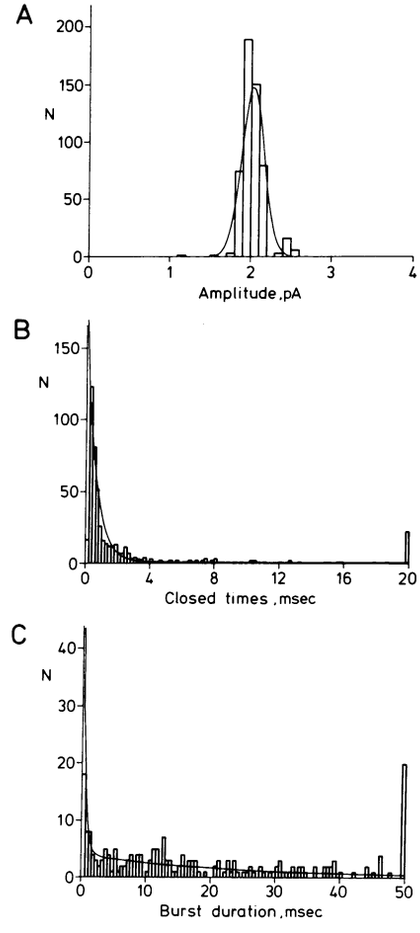

FIG. 5. Gating of GABA-activated channels. Outside-out patch recording with 50 μM GABA at a membrane potential of −70 mV. (*A*) Amplitude histogram of events has a single peak at 2.02 in this cell. (*B*) Histogram of closed time intervals. The distribution was fit by the sum of two exponentials with decay constants of 0.8 msec and 16.6 msec. The first bin was not used for the fit. From the area under the fast component, 374 short closings were observed. (*C*) Histogram of burst durations. Bursts were constructed as series of openings separated by time intervals of <1.6 msec. The distribution was fit by the sum of two exponentials with decay constants of 0.5 msec and 23.0 msec. The number of bursts (N) was 185.

which then converts to the open channel A_2R^*. This is in agreement with the Hill coefficient of ≈2 obtained from whole-cell dose–response curves. The short events in the burst-time distribution may reflect a population of openings arising from the monoliganded state of the receptor (4, 5, 20).

From our experimental results—i.e., the burst duration, the gap duration, and the number of gaps per burst—we could derive some of the rate constants in the above scheme (ref. 22 and see also ref. 6). The calculated rate constants are $\alpha = 140\ sec^{-1}$, $\beta = 833\ sec^{-1}$, and $k_{-1} = 208\ sec^{-1}$. Similar results were obtained from two other patches. These findings are consistent with those reported for GABA receptor channels in spinal (5) and hippocampal neurons (23) and also in chromaffin cells (6).

DISCUSSION

We have investigated whole-cell and single-channel currents activated by GABA in cultured astrocytes. Many properties of the glial GABA receptor resemble those reported for the neuronal $GABA_A$ receptor. The reversal potential of the GABA-activated whole-cell current was close to the Cl^- equilibrium potential, indicating that the channels are mainly permeable to Cl^- ions. The response to GABA increased approximately with the square of the GABA concentration. This finding indicates that at least two GABA molecules must bind to the receptor to open the channel. At GABA concentrations >10 μM, current amplitudes decreased in the presence of GABA as a consequence of receptor desensitization. These properties are identical to those reported for the neuronal GABA receptor (4, 6).

Analysis of single GABA-activated channels revealed further similarities between neuronal and glial GABA receptors. The astrocytic receptor channels displayed multiple conductance states of 12 pS, 21 pS, 29 pS, and 43 pS. The main-state conductance was consistently found to be 29 pS. The single-channel current–voltage relations were linear for all conductance states with a reversal potential close to the Cl^- equilibrium potential. Elementary current pulses appeared as bursts of openings. The time course of single-channel gating was similar to that described for neuronal cells (5, 6, 23).

GABA-activated whole-cell currents in astrocytes are modulated by benzodiazepine receptor ligands as described

for the GABA-induced membrane depolarization (14). Diazepam potentiated the GABA-activated current. The inverse benzodiazepine receptor agonist DMCM also slightly, but consistently, increased GABA-activated currents in astrocytes. This finding contrasts to results obtained in neurons and chromaffin cells. It indicates that the glial GABA–benzodiazepine receptor complex is in some respects different to its counterpart present in neurons.

In the astrocytes, we found two types of GABA-activated whole-cell currents. In some cells the noise of membrane current increased strongly in the presence of GABA and the currents developed rapidly. In another population of astrocytes, GABA-induced currents were not associated with an increase in membrane noise and the time course of activation was much slower. We never succeeded in recording single-channel currents from patches taken from the latter cell population, suggesting that GABA receptors are not uniformly distributed over the cell surface. It has been demonstrated for the nicotinic acetylcholine receptor that clustering of receptors can be induced by positively charged latex beads (24). A similar mechanism may be operative at glial membranes that are in contact with the poly(L-lysine) substrate or the glass surface. This would explain our finding that in one population of glia cells the currents developed much slower, possibly due to a hindered accessibility of GABA to its receptors.

It is tempting to speculate that glial GABA receptors are clustered at synaptic regions where astrocytic endfeet are found. This clustering of the receptor could be of functional importance. Assuming that it occurs at astrocytic membranes close to inhibitory synaptic regions, we propose a mechanism how glial cells could buffer Cl^- activity in the extracellular space (Fig. 6).

After the release of GABA from the presynaptic nerve terminal, postsynaptic GABA receptor channels are activated, which carry Cl^- ions from the extracellular space into the neuron, if the inhibitory postsynaptic potential is hyperpolarizing. As a consequence, the extracellular Cl^- concentration decreases as observed in slices from the CA1 and CA3 regions of the guinea pig hippocampus (25). With possibly a small delay, glial GABA receptors are activated in the vicinity of the synaptic cleft. The efflux of Cl^- and K^+ from glial cells (26) could be operative in rapidly restoring extracellular Cl^- and, in addition, may explain the depolarization

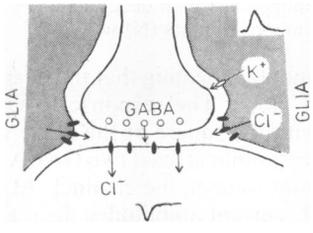

FIG. 6. Model of Cl^- regulation by glial cells at GABAergic synapses. The activation of postsynaptic GABA receptor channels is shown to induce a hyperpolarizing synaptic potential and an inwardly directed movement of Cl^- ions. Glial cells are depolarized by GABA. The efflux of Cl^- thus could buffer the loss of Cl^- from the extracellular space.

which follows the hyperpolarizing postsynaptic potential in neocortical neurons (27) and the delayed rise in extracellular Cl^- (25).

Thus, glial cells could have additional ion-regulatory functions besides their involvement in potassium homeostasis. The restoration of the neuronal Cl^- gradient during synaptic activity is an attractive mechanism by which glial cells may ensure the proper functioning of central inhibition.

We thank Drs. Bert Sakmann and Melitta Schachner for discussion and Frances Edwards for comments on the manuscript. This work was supported by the Deutsche Forschungsgemeinschaft (SFB 236 and 317, Heisenberg fellowship to H.K.) and the Bundesministerium für Forschung und Technologie.

1. Krnjević, K. & Schwartz, S. (1967) *Exp. Brain Res.* **3**, 320–336.
2. Barker, J. L. & Ransom, B. R. (1978) *J. Physiol. (London)* **280**, 331–354.
3. Bormann, J. (1988) *Trends Neurosci.* **11**, 112–116.
4. Bormann, J., Hamill, O. P. & Sakmann, B. (1987) *J. Physiol. (London)* **385**, 243–286.
5. Sakmann, B., Hamill, O. P. & Bormann, J. (1983) *J. Neural Transm. Suppl.* **18**, 83–95.
6. Bormann, J. & Clapham, D. E. (1985) *Proc. Natl. Acad. Sci. USA* **82**, 2168–2172.
7. Möhler, H. & Richards, J. G. (1981) *Nature (London)* **294**, 763–765.
8. Study, R. & Barker, J. L. (1981) *Proc. Natl. Acad. Sci. USA* **78**, 7180–7184.
9. Bormann, J., Ferrero, P., Guidotti, A. & Costa, E. (1985) *Regul. Peptides Suppl.* **4**, 33–38.
10. Gilbert, P., Kettenmann, H. & Schachner, M. (1984) *J. Neurosci.* **4**, 561–569.
11. Kettenmann, H., Backus, K. H. & Schachner, M. (1984) *Neurosci. Lett.* **52**, 25–29.
12. Kettenmann, H. & Schachner, M. (1985) *J. Neurosci.* **5**, 3295–3301.
13. Kettenmann, H., Backus, K. H. & Schachner, M. (1987) *Brain Res.* **404**, 1–9.
14. Backus, K. H., Kettenmann, H. & Schachner, M. (1988) *Glia* **1**, 132–140.
15. McCarty, K. D. & DeVellis, J. (1980) *J. Cell Biol.* **85**, 890–902.
16. Keilhauer, G., Meier, D., Kuhlmann, S. & Schachner, M. (1985) *EMBO J.* **44**, 2499–2504.
17. Fenwick, E. M., Marty, A. & Neher, E. (1982) *J. Physiol. (London)* **331**, 577–597.
18. Hamill, O. P., Marty, A., Neher, E., Sakmann, B. & Sigworth, F. J. (1981) *Pflügers Arch.* **312**, 85–100.
19. Sigworth, F. J. (1983) in *Single Channel Recording*, eds. Sakmann, B. & Neher, E. (Plenum, New York), pp. 301–321.
20. Colquhoun, D. & Sakmann, B. (1981) *Nature (London)* **294**, 464–466.
21. Del Castillo, J. & Katz, B. (1957)*Proc. R. Soc. London Ser. B* **146**, 369–381.
22. Colquhoun, D. & Hawkes, A. G. (1977) *Proc. R. Soc. London Ser. B* **199**, 231–262.
23. Sakmann, B., Bormann, J. & Hamill, O. P. (1983) *Cold Spring Harbor Symp. Quant. Biol.* **48**, 247–257.
24. Peng, H. B. & Cheng, P.-C. (1982) *J. Neurosci.* **2**, 1760–1774.
25. Müller, W., Misgeld, U. & Lux, H. D. (1988) *Pflügers Arch.* **411**, R149.
26. Kettenmann, H., Backus, K. H. & Schachner, M. (1988) in *Glial Cell Receptors*, ed. Kimelberg, H. K. (Raven, New York), pp. 95–106.
27. Deisz, R. A. & Prince, D. A. (1988) *J. Physiol. (London)*, in press.